X-ray magnetic circular dichroism study of the decoupling of the magnetic ordering of the Er and Co sublattices in $Er_{1-x}Y_xCo_2$ systems

J. Chaboy

Instituto de Ciencia de Materiales de Aragón, CSIC-Universidad de Zaragoza, 50009 Zaragoza, Spain

M. A. Laguna-Marco

CITIMAC, Universidad de Cantabria, Avda. de los Castros s/n, 39005 Santander, Spain

H. Maruyama, N. Ishimatsu, and Y. Isohama

Graduate School of Science, Hiroshima University, 1-3-1 Kagamiyama, Higashi-Hiroshima 739-8526, Japan

N. Kawamura

Japan Synchrotron Radiation Research Institute, 1-1-1 Kouto, Mikazuki, Sayo, Hyogo 679-5148, Japan

We present an x-ray magnetic circular dichroism (XMCD) study performed at the Co K edge and at the Er $L_{2,3}$ edges in the $Er_{1-x}Y_xCo_2$ series. Our results indicate that both Er and Co magnetic sublattices order at the same temperature for all the investigated compounds. In the case of the $Er_{0.6}Y_{0.4}Co_2$ compounds, XMCD data do not show the decoupling of the magnetic ordering for both Er and Co sublattices. Moreover, no experimental evidence of the occurrence of an inverse itinerant electron metamagnetism has been found for applied magnetic fields of up to $\mu_0H = 10$ T. In addition, a nonzero magnetic moment is found at the Co sites in the case of the $Er_{0.5}Y_{0.5}Co_2$ compound.

PACS number(s): 75.30.Kz, 61.10.Ht

I. INTRODUCTION

The intermetallic RCo_2 compounds (R stands for rare-earth elements) are of particular interest among the intermetallic rare-earth compounds with $3d$ transition metals. In the case of the isostructural RNi_2 and RFe_2 compounds the $3d$ subsystem is, respectively, nonmagnetic or bearing a stable magnetic moment. By contrast, it shows an intermediate behavior in the RCo_2 case. The RCo_2 compounds are characterized by both the dependence of the Co magnetic moment upon the R alloying component and the occurrence of a metamagnetic transition in the Co $3d$ itinerant subsystem. For compounds in which R is nonmagnetic (YCo_2, $LuCo_2$) the Co susceptibility is of the Pauli type, while a $\sim 1\mu_B$ Co moment is induced in the case of compounds with magnetic R metals. In the latter case, the magnetic order of the d subsystem is due to the effect of the molecular field created by the R moments and acting on the Co sites.

The RCo_2 compounds have been widely studied as they can be regarded as model materials for a large variety of magnetic phenomena related with the itinerant electron metamagnetism (IEM).[1–4] This long-standing interest is still open as new magnetic properties have been discovered during this research. This is the case of the magnetic characterization of the $Er_{1-x}Y_xCo_2$ systems. These systems were tailored to study the modification of the IEM behavior associated with the reduction of the molecular field acting on the Co atoms by substituting Er by a nonmagnetic rare-earth element such as Y. The electronic and magnetic properties of the $Er_{1-x}Y_xCo_2$ systems were earlier studied by Duc *et al.*,[5] who found that the magnetic moment of Co atoms decreases with decreasing Er content, as does the Curie temperature. These authors concluded that the induced character of the Co mag-

netic moment and, in addition, the character of the magnetic transition change from first to second order around $x = 0.3$.[5] Later, neutron diffraction experiments performed by Baranov *et al.*[6] show that an increase of the yttrium concentration will cause a sharp drop in μ_{Co} and μ_{Er}. These studies also emphasize the coexistence of both long-range and short-range order for yttrium concentrations close to the critical one where the long-range magnetic order disappears. According to the results by Baranov *et al.* the sharp drop in μ_{Co} starts for $x > 0.4$ and there is no short-range ordering for $x > 0.6$ down to $T = 4.2$ K.[6]

More recently, Hauser *et al.* have proposed that for a certain yttrium concentration $x = 0.4$, the magnetic ordering of the Er and Co sublattices takes place at different temperatures.[7–10] This result is mainly based on specific heat capacity measurements of $Er_{0.6}Y_{0.4}Co_2$ showing two anomalies with maxima at $T = 11$ K and 14.5 K.[7,9] According to these authors the Er sublattice magnetically orders at $T = 14.5$ K, but as the molecular field acting on the Co atoms is smaller than the critical one, the Co sublattice remains magnetically disordered. The critical condition for the onset of magnetic order in the Co subsystem is fulfilled on cooling, thus resulting in a second transition when a magnetic moment is induced at the Co sites at $T = 11$ K. However, the striking result that the itinerant Co sublattice orders at a lower temperature than the Er sublattice has not been confirmed by recent neutron studies. In particular, single-crystal neutron diffraction experiments on $ErCo_2$ and $Er_{0.6}Y_{0.4}Co_2$ showed that both Er and the Co magnetic sublattices order at the same temperature (35.9 and 17.0 K, respectively).[11,12] Moreover, macroscopic data on single-crystal specimens do not show two separate peaks neither for the specific heat or for the magnetic susceptibility, in disagreement with the ex-

TABLE I. Structural and magnetic parameters of the $Er_{1-x}Y_xCo_2$ compounds: lattice constant (a), Curie temperature (T_C), magnetization measured at 5 T (M_{5T}), and the Co moment derived from the magnetization data at $\mu_0 H = 5$ T.

Compound	a (Å)	T_C (K)	M_{5T} (μ_B/f.u.)	μ_{Co} (μ_B/f.u.)
$x = 0$	7.157	32	7.2	0.9
$x = 0.2$	7.166	23.5	5.8	0.7
$x = 0.3$	7.173	18.5	4.9	0.7
$x = 0.4$	7.177	15	4.3	0.55
$x = 0.5$	7.190	12	3.7	0.4
$x = 0.6$	7.192	8.5	3.0	0.3

periments on polycrystalline materials reported by Hauser *et al.*[7,9] This controversy extends also to other results as the so-called inverse IEM transition. This transition is induced by increasing the external field, as the effective field acting upon the Co subsystem decreases and the Co moment abruptly collapses. In the case of $Er_{0.6}Y_{0.4}Co_2$ the inverse IEM transition occurs at 8.5 T.[4,10] However, Markosyan *et al.* have reported this value to be 7 T, being reduced with pressure so as to vanish above a critical value of 2 kbar.[13] By contrast, results by Podlesnyak *et al.* indicate that no inverse IEM is observed under pressures of up to 6 kbar.[11] Finally, contradictory results are also reported for the magnetic behavior of the $Er_{1-x}Y_xCo_2$ compounds near the critical yttrium concentration for the occurrence of long-range magnetic order. While several authors suggest the coexistence of both long-range and short-range order,[6,11,14] other works indicate that for $Er_{0.5}Y_{0.5}Co_2$ only the Er sublattice is magnetically ordered although the Co subsystem is still affected by the molecular field and a $0.22\mu_B$ moment at the Co sites is reported.[9]

Aimed to clarify this debate we have performed an x-ray magnetic circular dichroism (XMCD) study at the Co K edge and at the Er $L_{2,3}$ edges in the $Er_{1-x}Y_xCo_2$ series. This XMCD approach furnishes a disentangled magnetic characterization of both Er and Co sublattices by studying the variation of the XMCD as a function of the yttrium concentration, the applied magnetic field, and the temperature.

II. EXPERIMENT

$Er_{1-x}Y_xCo_2$ ($x = 0$, 0.2, 0.3, 0.4, 0.5, and 0.6) samples were prepared by arc-melting the pure elements under Ar protective atmosphere. The ingots were annealed in evacuated quartz tubes at 850 °C for one week. Structural characterization was performed at room temperature by means of powder x-ray diffraction, by using a rotating-anode Rigaku diffractometer in the Bragg-Brentano geometry, with Cu $K\alpha$ radiation. The diffraction patterns, Rietveld-refined using the FULLPROF code,[15] showed that all the samples show a single C15 Laves phase, being the presence of secondary phases less than <2% overall. The cell parameters determined from the XRD patterns are summarized in Table I. Magnetization measurements were performed by using a commercial superconducting quantum interference device (SQUID) magneto-

meter (Quantum Design MPMS-S5) in magnetic fields up to 5 T.

XMCD experiments were performed at the beamline BL39XU of the SPring8 Facility.[16] XMCD spectra were recorded in the transmission mode at both the Co K edge and Er $L_{2,3}$ edges using the helicity-modulation technique.[17] For the measurements, homogeneous layers of the powdered samples were made by spreading of fine powders of the material on an adhesive tape. The thickness and homogeneity of the samples were optimized to obtain the best signal-to-noise ratio, giving a total absorption jump ~ 1 at about 100 eV above the edge. The XMCD spectra were recorded at fixed temperatures and under the action of an applied magnetic field of up to 10 T. The spin-dependent absorption coefficient was then obtained as the difference of the absorption coefficient $\mu_c = (\mu^- - \mu^+)$ for antiparallel, μ^-, and parallel, μ^+, orientation of the photon helicity and sample magnetization. The origin of the energy scale, E_0, was chosen in all the cases at the inflection point of the absorption edge.

III. RESULTS AND DISCUSSION

A. Macroscopic magnetic measurements

The temperature dependence of the magnetization of the $Er_{1-x}Y_xCo_2$ series is shown in Fig. 1. For both $ErCo_2$ and $Er_{0.8}Y_{0.2}Co_2$ compounds, the variation of the magnetization at the onset of the magnetic ordering temperature T_C proceeds steplike, as corresponding to the first-order character of the transition. However, for higher yttrium contents the change of the magnetization proceeds smoothly, indicating that the transition becomes second order.[5] Magnetization versus applied magnetic field curves recorded at $T = 5$ K (see Fig. 1) show the progressive reduction of the magnetization as the Y content increases, although ferrimagnetic behavior is retained. Assuming the free-ion value ($9\mu_B$) to the erbium moment and that μ_{Er} is not affected by the yttrium substitution,[5,18] μ_{Co} in the $Er_{1-x}Y_xCo_2$ series is determined to decrease from $\sim 0.9\mu_B$ in $ErCo_2$ to 0.3 in $Er_{0.4}Y_{0.6}Co_2$.

The magnetic behavior of the $Er_{0.6}Y_{0.4}Co_2$ compound deserves a special discussion. Hauser *et al.* have proposed that the magnetic ordering of both the Er and Co magnetic sublattices take place at different temperatures.[7,9] This result is mainly based in the appearance of two anomalies in C_p measurements of polycrystalline samples. The thermal dependence of C_p is similar to that early reported by Duc *et al.*, although the above referred anomalies were not detected.[5] Indeed, recent measurements on a $Er_{0.6}Y_{0.4}Co_2$ single crystal do not show separate peaks either for the specific heat or for the magnetic susceptibility.[12] In addition to the C_p anomalies, Hauser *et al.* argue that evidence of different ordering temperatures for the Er and Co subsystems in $Er_{0.6}Y_{0.4}Co_2$ can be found in the behavior of the magnetization.[9] In this way, M vs T curves of $Er_{0.6}Y_{0.4}Co_2$ cooled under an applied 1 mT field show two smooth steps that are interpreted as due to two separate magnetic transitions. However, this interpretation of the magnetization data for such a small external field (1 mT) is not free of controversy as the effect of the microstructure, coercivity and the domain structure of the polycrystalline samples is not considered. Indeed, the double-step
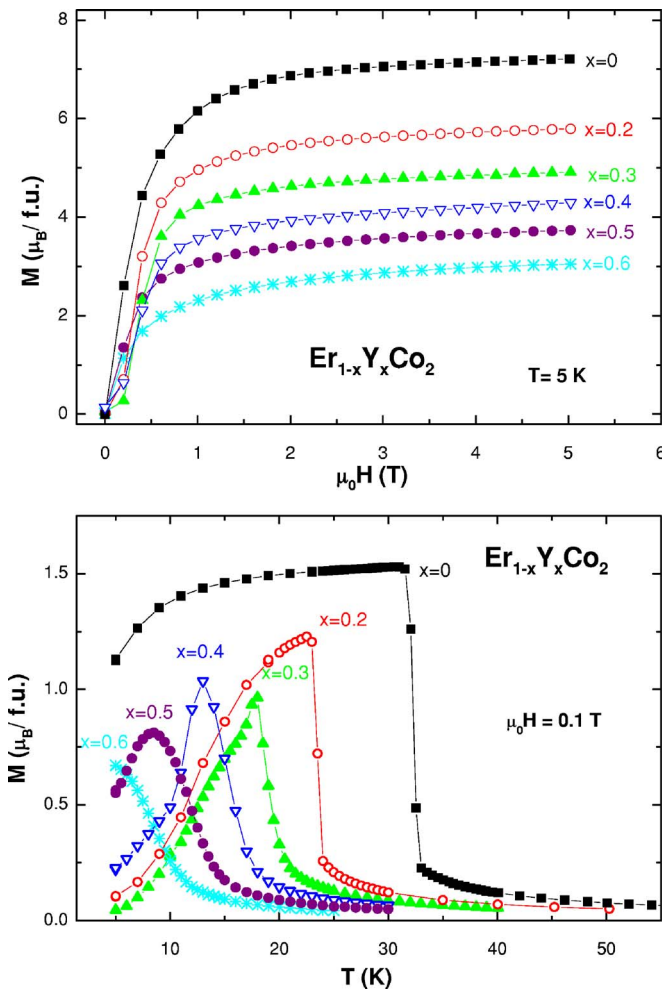
FIG. 1. (Color online) Thermal dependence of the magnetization (zero field cooled) of the $Er_{1-x}Y_xCo_2$ compounds: $x=0$ (■), 0.2 (○, red), 0.3 (▲, green), 0.4 (▽, blue), 0.5 (•, purple), and 0.6 (∗, cyan). In the top panel, magnetization vs applied magnetic field curves recorded at $T=5$ K are shown.

feature of the field-cooled (FC) magnetization can be observed for higher applied fields of up to 0.1 T (see Fig. 2). However, as the external magnetic field is increased the anomalies disappear, which is difficult to reconcile with the expected behavior of the external field on the IEM transitions. According to the mean-field approach, the cobalt moment in RCo_2 systems is induced by the molecular field on the Co atoms, B_{mol}^{Co}, exerted by the localized $4f$ moments. The direction of B_{mol}^{Co} is antiparallel to that of the Er moment and, hence, to that of the applied magnetic field. Consequently, the effective field acting upon the Co subsystem decreases with increasing the external field: $B_{eff}^{Co}=B_{mol}^{Co}-B_{ext}$. Moreover, if B_{ext} exceeds a critical field B_{cr}, the Co sublattice magnetization is destabilized and the Co moment abruptly collapses in the so called inverse IEM transition. Consequently, contrary to the observed results, the effect of increasing the magnetic field in the presence of two separate transitions would enhance the different temperature ordering of both the Er and Co sublattices. It can be argued to account for such a disagreement that upon increasing the field the Er magnetization increases in such a way that the second tran-

sition is favored and coupled to that of the Er sublattice. However, it is difficult to reconcile this picture with the M vs H behavior. As shown in Fig. 2, the magnetization at low and moderate applied fields ($\mu_0 H \lesssim 2$ T) is always smaller at 13 K than at $T=11$ K. By contrast, if the Co sublattice orders ferrimagnetically coupled to that of Er at $T=11$ K, one expects a decrease of the magnetization that is not observed.

Consequently, the magnetic characterization of $Er_xY_{1-x}Co_2$ compounds shows contradictory results even when the same experimental techniques are used. This controversy specially regards the decoupling of the magnetic ordering of the Er and Co sublattices near the critical yttrium concentration for the onset of long-range magnetic ordering.[6–12,14] Trying to get a deeper insight into this debate we have extended our study by using XMCD at the Co K edge and at the Er $L_{2,3}$ edges. In this way, the element-selectivity properties of XMCD can provide a magnetic characterization of the systems in which the magnetic behavior of both the Co and Er sublattices are disentangled.

B. Er L_3 edge XMCD

The Er L_3 edge XMCD spectra of several $Er_{1-x}Y_xCo_2$ compounds are shown in Fig. 3. These spectra are characterized by a negative peak (A) below the edge (~-5 eV) and a main positive peak (B) at ~3 eV above the edge. These structures have been interpreted as due to both a quadrupolar and dipolar transition, respectively.[19] Consequently, the low-energy feature is influenced by the localized Er $4f$ states while the high-energy feature is linked to the magnetic behavior of the conduction $5d$ states. For all the investigated $Er_{1-x}Y_xCo_2$ compounds the amplitude of the Er L_3 XMCD signal is smaller than that obtained for $ErAl_2$. This result can be interpreted in terms of a reduction of the Er magnetic moment in the case of the Co-containing samples with respect the Er free-ion value that is assigned to the $ErAl_2$ compound.[20] However, the intensity of the main XMCD features (A and B) presents a different dependence on the Y content through the $Er_{1-x}Y_xCo_2$ series. In particular, the intensity of feature B is similar for both $Er_{0.6}Y_{0.4}Co_2$ and $Er_{0.5}Y_{0.5}Co_2$ compounds, being significantly smaller ($\sim20\%$) for $ErCo_2$. By contrast, the peak-A intensity is near the same for the three cobalt compounds.

In a first approach, one can consider that the intensity of the quadrupolar peak is, to some extent, reflecting the $4f$ Er magnetic moment being the same for the three investigated compounds. The modification of the dipolar contribution, peak B, can be addressed by two different effects. On the one hand, it can be simply interpreted in terms of the reduction of the Er $5d$ moment in $ErCo_2$ with respect to that in the Y-doped compounds. However, this interpretation is in conflict with the expected behavior for the $Er_{1-x}Y_xCo_2$ compounds, as the Er-Y substitution leads to the relaxation of the magnetic ordering within the rare-earth magnetic sublattice. On the other hand, recent results obtained in Al-doped RFe_2 series indicates that the transition metal contributes, with contrary sign, to the XMCD signals recorded at the rare-earth L edges.[21] Accordingly, the dipolar contribution of the Er L_3 XMCD signal is made up by the addition of both the Er and
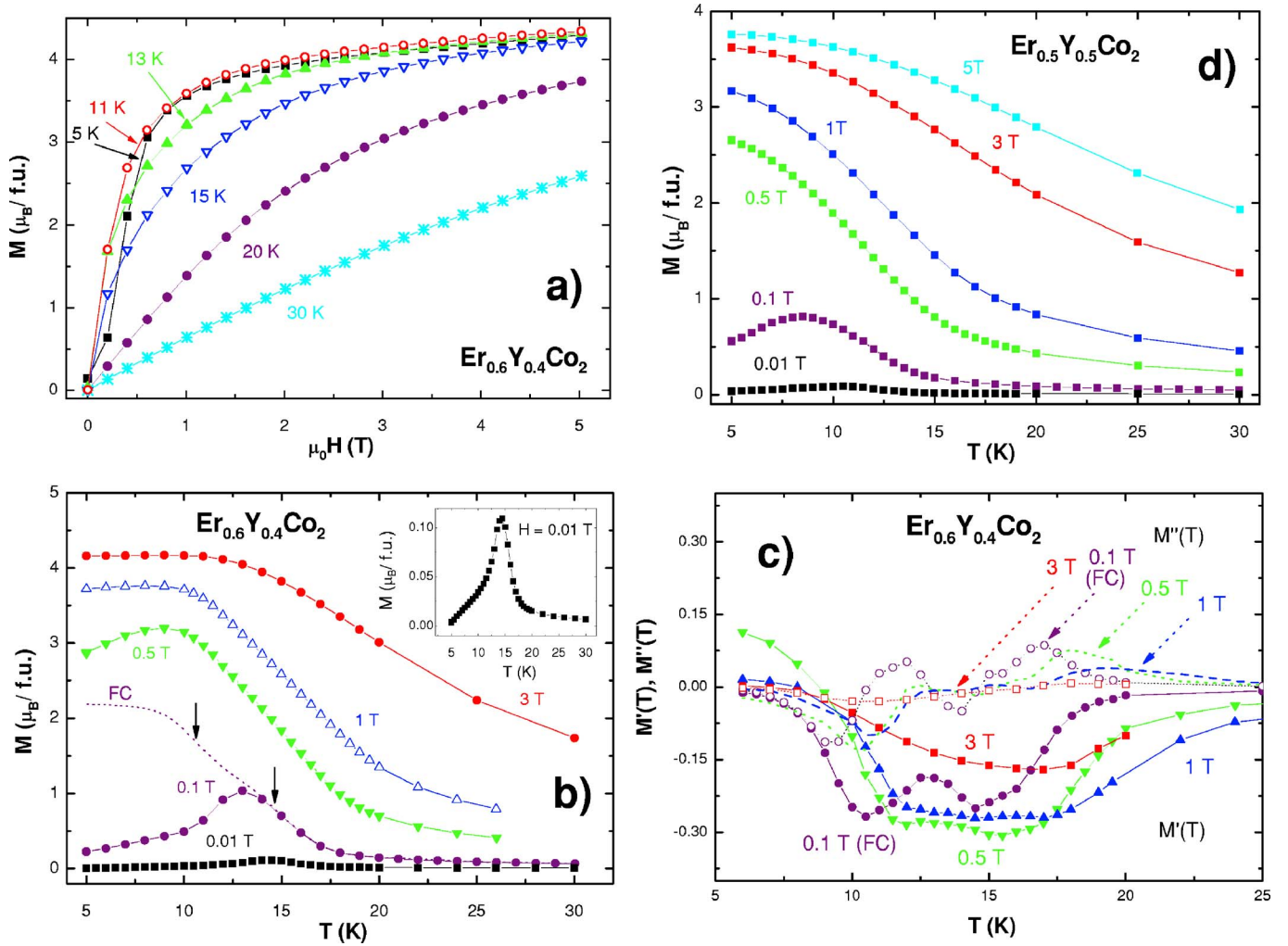
FIG. 2. (Color online) (a) Magnetization vs applied magnetic field curves of $Er_{0.6}Y_{0.4}Co_2$ recorded at different temperatures: $T=5$ K ($\blacksquare$), 11 K ($\bigcirc$, red), 13 K ($\blacktriangle$, green), 15 K ($\triangledown$, blue), 20 K ($\bullet$, purple), and 30 K ($*$, cyan). (b) Zero-field-cooled magnetization vs temperature curves of $Er_{0.6}Y_{0.4}Co_2$ recorded at different applied magnetic fields: $\mu_0H=3$ T ($\bullet$, red), 1 T ($\triangle$, blue), 0.5 T ($\blacktriangledown$), 0.1 T ($\bullet$, purple), and 0.01 T ($\blacksquare$). In the case of $\mu_0H=0.1$ T the field-cooled curve is also reported (dotted line) and the arrows mark the steplike features discussed in the text. The inset reports a detailed view of $M(T)$ at $\mu_0H=0.01$ T. (c) First and second derivatives of the $M(T)$ curves of $Er_{0.6}Y_{0.4}Co_2$ recorded at different applied magnetic fields. (d) Zero-field-cooled magnetization vs temperature curves of $Er_{0.5}Y_{0.5}Co_2$ recorded at different applied magnetic fields.

Co contributions. The reduction of the intensity of peak *B* in $ErCo_2$ as compared to both $Er_{0.6}Y_{0.4}Co_2$ and $Er_{0.5}Y_{0.5}Co_2$ indicates that the Co contribution is more important in the pure compound than in the Y-doped ones. This contribution being related to the Co magnetic moment, this result indicates that μ_{Co} decreases in the Y-substituted samples, in agreement with the behavior derived from the magnetization data. Within the experimental resolution, the XMCD signal of $Er_{0.5}Y_{0.5}Co_2$ is slightly greater than the $Er_{0.6}Y_{0.4}Co_2$ one, in agreement also with the observed variation of μ_{Co} as a function of the Y content.

Figure 4(a) reports the comparison of the Er L_3-edge XMCD spectra of $Er_{0.6}Y_{0.4}Co_2$ recorded at different applied magnetic fields and at two different temperatures $T=13$ K and $T=5$ K. According to Hauser *et al.*, the Er sublattice magnetically orders at $T_{Er}=14.5$ K, while the onset of magnetic order in the *d* subsystem takes place for a lower T_{Co} = 11 K temperature.[7–9] Based on the above results, one ex-

pects that Er L_3-edge XMCD recorded at temperatures T_{Co} $<T<T_{Er}$ and $T<T_{Co}$ reflects the different magnetic ordering of the Co sublattice. However, the shape of the XMCD is similar for both temperatures. Indeed, as shown in Fig. 4(b), the signals obtained at $T=5$ K can be reconstructed by using a scaling factor from those recorded at $T=13$ K by applying the same magnetic field. The scaling factor needed to match both signals is ~1.4 for low applied fields, while it reaches ~1.1 for $\mu_0H=5$ T. This behavior is similar to that exhibited by the $M(H)$ curves at the same temperatures. At the maximum applied field $\mu_0H=5$ T, the magnetization of $Er_{0.6}Y_{0.4}Co_2$ is near the same for both temperatures. By contrast, for applied fields of $\mu_0H=0.5$ T and 1 T it is necessary to apply a constant enhancing factor (~1.1) to the $M(H)$ values recorded at $T=13$ K to match those found at $T=5$ K.

As shown in Fig. 4(b) the agreement between the XMCD spectra recorded at $T=5$ K and those scaled from the T = 13 K ones concerns both the low-energy (*A*) and the edge
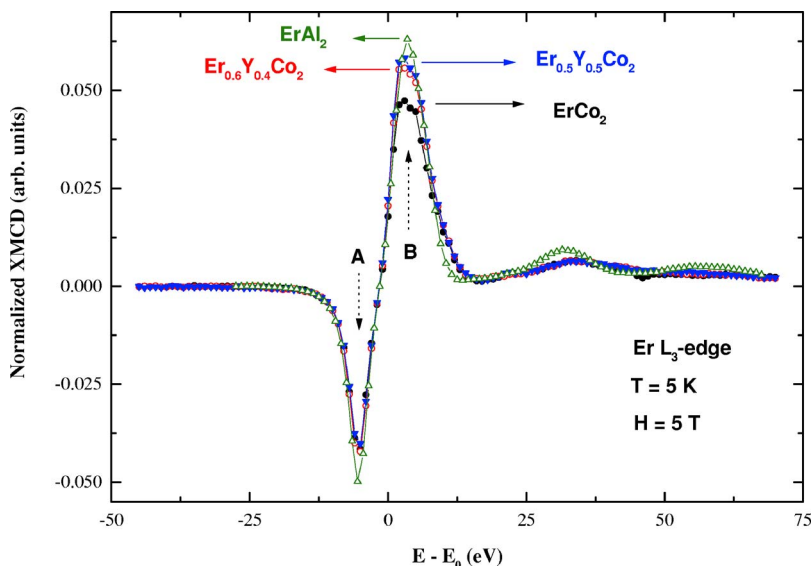
FIG. 3. (Color online) Comparison of the Er L_3-edge XMCD spectra recorded at $T=5$ K and $\mu_0 H=5$ T in the case of $ErAl_2$ (green, $\triangle$), $ErCo_2$ (black, •), $Er_{0.6}Y_{0.4}Co_2$ (red, $\bigcirc$), and $Er_{0.5}Y_{0.5}Co_2$ (blue, $\bigtriangledown$).
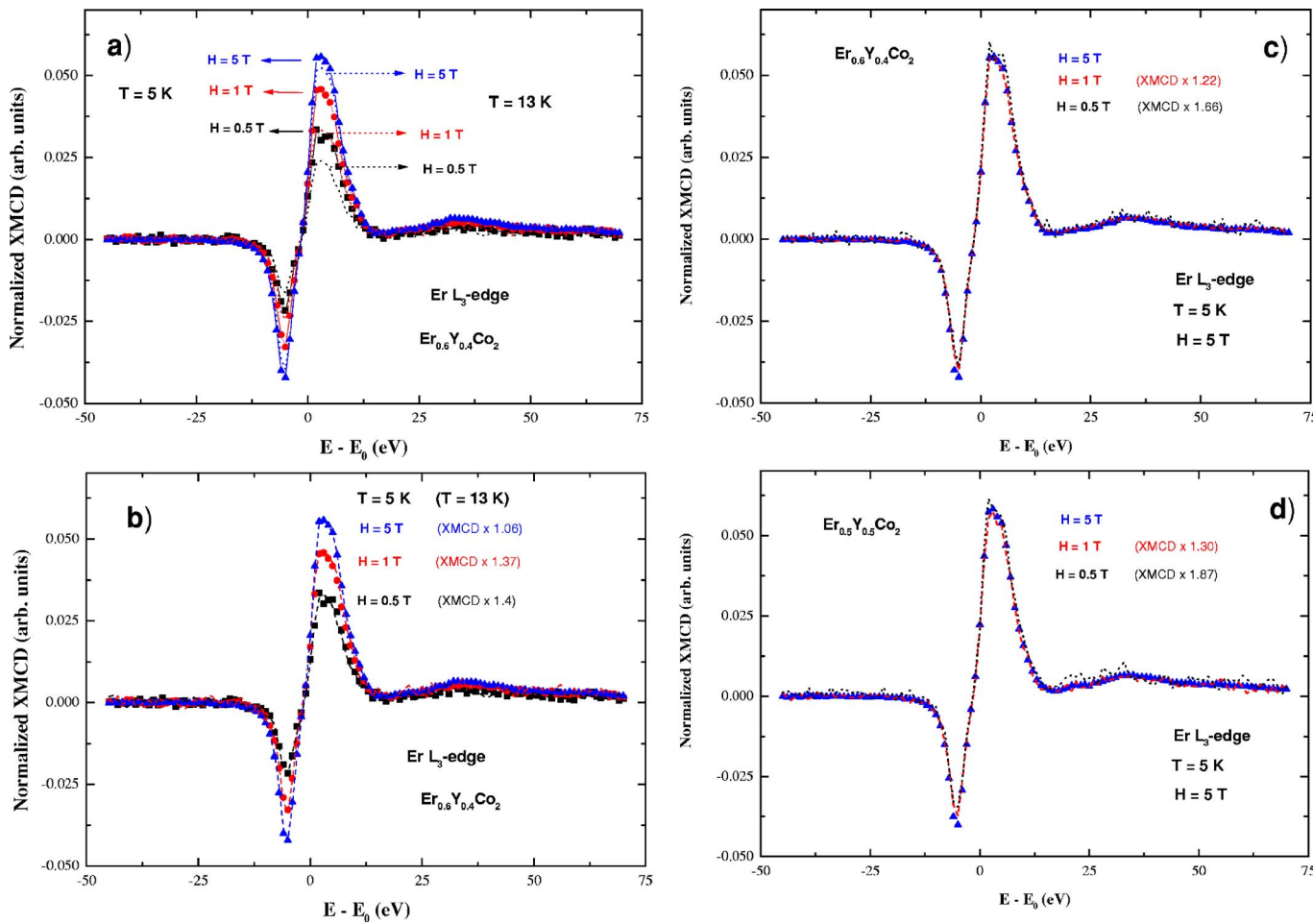

FIG. 4. (Color online) (a) Comparison of the Er L_3-edge XMCD spectra of $Er_{0.6}Y_{0.4}Co_2$ recorded at $T=5$ K at different applied magnetic fields: $\mu_0 H=0.5$ T (■), 1 T (red, •), and 5 T (blue, $\triangle$). The dotted lines show the same comparison for the spectra recorded at $T=13$ K. (b) Comparison of the Er L_3-edge XMCD spectra of $Er_{0.6}Y_{0.4}Co_2$ recorded at $T=5$ K and different $\mu_0 H$ (symbols) and those obtained (see text for details) scaling the XMCD recorded at the same fields at $T=13$ K (dotted lines). (c) and (d) panels show the comparison of the Er L_3-edge XMCD spectrum recorded at $T=5$ K and $\mu_0 H=5$ T (blue, $\triangle$) and those obtained by scaling the spectra recorded at $\mu_0 H=1$ T (red, dashed) and 0.5 T (black, dotted) in the case of $Er_{0.6}Y_{0.4}Co_2$ (c) and $Er_{0.5}Y_{0.5}Co_2$ (d).
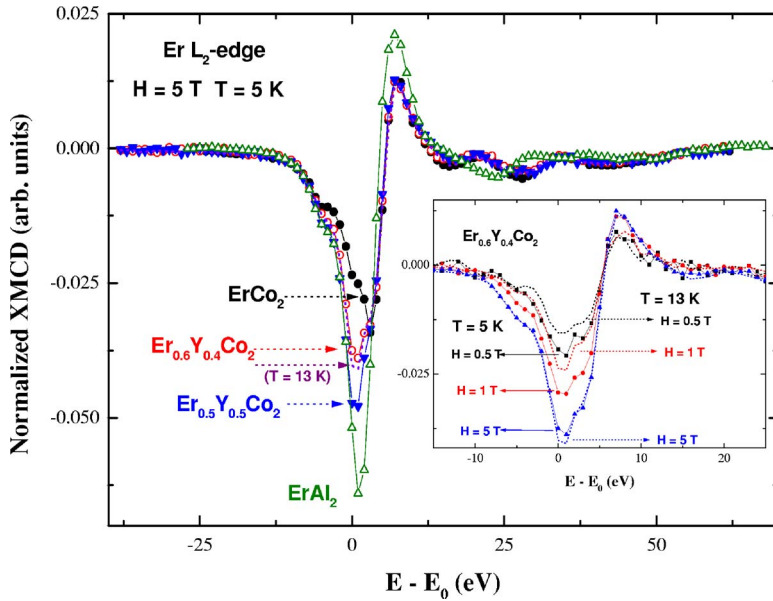
FIG. 5. (Color online) Comparison of the Er L_2-edge XMCD spectra in the case of $ErAl_2$ (green, △), $ErCo_2$ (black, •), $Er_{0.6}Y_{0.4}Co_2$ (red, ○), and $Er_{0.5}Y_{0.5}Co_2$ (blue, ▽) recorded at T =5 K and $\mu_0 H$=5 T. The XMCD spectrum of $Er_{0.6}Y_{0.4}Co_2$ recorded at T=13 K is also shown (purple, dotted line). The inset shows the comparison of the Er L_2-edge XMCD spectra of $Er_{0.6}Y_{0.4}Co_2$ recorded at T=5 K at different applied magnetic fields: $\mu_0 H$=0.5 T (■), 1 T (red, •), and 5 T (blue, △). The dotted lines show the same comparison for the spectra recorded at T =13.

(B) main spectral features. Peak A being addressed to Er and peak B reflecting the contribution of both Er and Co sublattices, these results seem to indicate that the magnetic state of the cobalt sublattice in $Er_{0.6}Y_{0.4}Co_2$ is the same at both temperatures; i.e., the Co sublattice orders at the same temperature as the Er one does. This behavior does not depend on the applied magnetic field. Indeed, the effect of the field only affects the amplitude of the spectra being the shape unaltered by varying the applied field. As shown in Fig. 4(c) the XMCD spectrum recorded at $\mu_0 H$=5 T is reproduced by those recorded at $\mu_0 H$=0.5 T and 1 T by using a scaling factor of 1.7 and 1.2, respectively. These scaling factors coincide with those needed to match the macroscopic $M(H)$ values at the same applied fields. Interestingly, the same behavior is observed for the $Er_{0.5}Y_{0.5}Co_2$ compound [Fig. 4(d)]. According to Hauser *et al.* only the Er sublattice is magnetically ordered in this compound. However, the XMCD results indicate that the behavior of both $Er_{0.5}Y_{0.5}Co_2$ and $Er_{0.6}Y_{0.4}Co_2$ is similar, thus supporting the conjecture that in the x=0.5 compound Co atoms also carry a magnetic moment and that both Er and Co sublattices are magnetically ordered.

C. Er L_2-edge XMCD

The results obtained from the Er L_3-edge XMCD can be corroborated by studying the evolution of the Er L_2-edge XMCD spectra throughout the $Er_{1-x}Y_xCo_2$ series. In this way, we present in Fig. 5 the comparison of the XMCD spectra recorded for the Co-containing samples and for reference $ErAl_2$. As shown in the figure, the spectral profile of the Er L_2-edge spectrum of $ErAl_2$ consists of a main negative peak centered at ~1 eV above the edge and a positive peak of lower intensity at E=7 eV. In the case of the Co samples, the shape of the positive structure remains unaltered and all the samples show a similar intensity. However, the main negative feature is strongly modified, in both shape and intensity, with respect to that of $ErAl_2$. For the $ErCo_2$ XMCD

spectrum the negative peak splits, the position of the minimum is shifted towards higher energy, and its intensity decreases. As a result one finds that the amplitude of the Er L_2-edge XMCD signal of $ErCo_2$ is about half of that of $ErAl_2$. According to macroscopic data, such a strong difference cannot be accounted in terms of the reduction of the Er magnetic moment. It is therefore necessary to appeal to the existence of additional contributions, other than the Er magnetization itself, to account for the observed behavior of the XMCD signals. In this respect, recent results obtained on R-Fe intermetallic compounds have demonstrated the existence of an extra contribution at the rare-earth L_2-edge XMCD spectra that is connected to the presence of Fe.[21,22] Consequently, the XMCD results reported Fig. 5 indicate that Co is contributing to the Er L_2 dichroism even when Er is probed. This cobalt contribution can be extracted by subtracting both $ErAL_2$ and $ErCo_2$ spectra yielding, as in the case of R-Fe systems,[21,22] a positive contribution.

This finding allows us to understand the evolution of the Er L_2-edge XMCD spectra as Y content increases through the $Er_{1-x}Y_xCo_2$ series. As shown in Fig. 5, the intensity of the negative peak of the XMCD spectra increases as Y does. In this way, the shape of the signal for $Er_{0.5}Y_{0.5}Co_2$ looks closer to that of $ErAl_2$, while that of $Er_{0.6}Y_{0.4}Co_2$ lies in between the $ErCo_2$ and $ErAl_2$ ones. According to the hypothesis above, Co is contributing with positive sign to the region of the spectrum where the main negative peak lies. As a result, the peak is strongly depressed for $ErCo_2$. As Co magnetic moment decreases, its contribution to the spectrum does too and consequently the negative intensity of this spectral feature is enhanced. Then, this behavior indicates that (i) as Y content increases the Co moment decreases and (ii) a Co moment is present in the case of both $Er_{0.6}Y_{0.4}Co_2$ and $Er_{0.5}Y_{0.5}Co_2$ compounds. The reduction of μ_{Co} has been estimated in the following way: we have assigned that the difference of the XMCD at E=1 eV between $ErCo_2$ and $ErAl_2$ is proportional to μ_{Co}, that according to magnetization data is ~0.9μ_B at T=5 K and $\mu_0 H$=5 T. In the case of $Er_{0.6}Y_{0.4}Co_2$ and $Er_{0.5}Y_{0.5}Co_2$ the difference is only the 64%
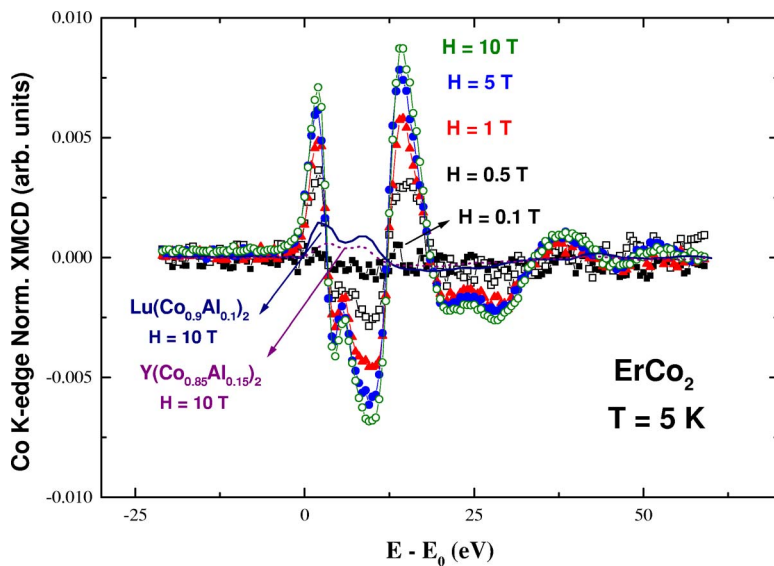
FIG. 6. (Color online) Comparison of the Co K-edge XMCD spectra of ErCo$_2$ recorded at T = 5 K and different applied magnetic fields: $\mu_0 H$ = 0.1 T (■), 0.5 T (black, ■), 1 T (red, △), 5 T (blue, •), and 10 T (green, ○). For the sake of comparison the XMCD spectra of Y(Co$_{0.85}$Al$_{0.15}$)$_2$ (purple, dotted line) and Lu(Co$_{0.9}$Al$_{0.1}$)$_2$ (navy, solid line) recorded at $\mu_0 H$ = 10 T and T = 5 K are also shown.

and 41%, respectively, of that of ErCo$_2$. Accordingly, the Co magnetic moments derived from the Er L_2-edge XMCD are 0.58μ_B and 0.37μ_B for Er$_{0.6}$Y$_{0.4}$Co$_2$ and Er$_{0.5}$Y$_{0.5}$Co$_2$, respectively, being in good agreement with the values, 0.55μ_B and 0.4μ_B, derived from the magnetization data reported in Table I.

A final study is deserved to the thermal dependence of μ_{Co} in Er$_{0.6}$Y$_{0.4}$Co$_2$. Accordingly to the analysis above, the comparison between the XMCD signals recorded at T = 13 K and T = 5 K, shown in Fig. 5, indicates that an ordered magnetic moment on Co sites exists at both temperatures. This result is in agreement with that obtained at the Er L_3 edge. However, because several works suggest that the onset of magnetic order in the Co sublattice is decoupled from the Er one and it takes place at T_{Co} = 11 K,[7–9] we have further verified this finding by recording the XMCD at different magnetic applied fields. As shown in Fig. 5 (inset), the XMCD spectra recorded at T = 13 K—i.e., at temperatures above the proposed one for the onset of Co magnetic ordering—are similar to those obtained at T = 5 K—i.e., when both sublattices are ordered. The dependence of the XMCD intensity on the applied magnetic field resembles, for both temperatures, the behavior of the $M(H)$ curves. Consequently, these results indicate that the Co sublattice orders at the same temperature as the Er one does.

D. Co K-edge XMCD

Our main aim being to determine if the magnetic ordering or the Er and Co sublattices of Er$_{0.6}$Y$_{0.4}$Co$_2$ are decoupled[7–10] or not[11,12] one can to think that the study of Co K-edge XMCD can offer a direct answer to this debate. In this way, the analysis of the temperature dependence of the Co K-edge XMCD would be preferable of using an indirect, but precise, way of studying the Co contribution to the Er $L_{2,3}$-edge XMCD spectra to solve the problem. However, the analysis of the Co K-edge in R-Co intermetallic compounds is nowadays an open task.

Previous works performed on R-Fe intermetallic compounds have unambiguously determined that there is a rare-earth contribution to the Fe K-edge XMCD reflecting the magnetic state of the R atoms.[22–26] Similar result has been obtained at the Co K-edge XMCD spectra of TbCo$_5$, Dy(Ni$_{0.2}$Co$_{0.8}$)$_5$, and TbCo$_2$ compounds.[27] The systematic research performed on the R-Fe compounds has determined that this rare-earth contribution depends on the R:Fe ratio in such a way that by increasing the number of rare-earth neighbors around the absorbing Fe atom its influence on the Fe K-edge XMCD spectrum is enhanced. Throughout all the studied series (RFe$_{11}$Ti,[26] R_2Fe$_{14}$B,[23–25] R_6Fe$_{23}$[22] and RFe$_2$[28]) the maximum contribution is found for the RFe$_2$ Laves compounds.

The presence of such an additional R contribution makes difficult the analysis of the Fe K-edge XMCD spectra in the R-Fe intermetallics. However, it is possible to disentangle both the Fe and R components to the spectrum by performing a two-sublattice analysis assuming the additivity of the Fe and R magnetic contributions to the XMCD. In the case of R-Fe intermetallics, this disentangling is also favored because the iron contribution to the Fe K-edge XMCD spectrum closely resembles that of Fe metal. It shows a narrow positive peak at the absorption threshold and a broad negative dip ($\sim$12 eV wide) at high energies, where the rare-earth contribution is mainly located. This main peak can be used in most cases as a fingerprint to determine the Fe contribution.[29] By contrast, such a feature is absent in the Co K-edge XMCD of R-Co compounds and both Co and R contributions are mixed throughout the whole energy range. Moreover, in the case of the RCo$_2$ Laves compounds the rare-earth contribution is so intense as to completely hinder the Co one.

This is illustrated in Fig. 6, where the Co K-edge dichroism of ErCo$_2$ is compared to that of Y(Co$_{0.85}$Al$_{0.15}$)$_2$ and Lu(Co$_{0.9}$Al$_{0.1}$)$_2$. In the latter case the rare-earth contribution to the XMCD is absent as the rare earth is nonmagnetic. In a first approach, one can considers that the Co K-edge XMCD of these compounds reveals the contribution of the cobalt sublattice Co to the Co K-edge spectrum XMCD of the RCo$_2$ compounds in which R is magnetic. As shown in the figure, the amplitude of the XMCD is one order of magnitude larger
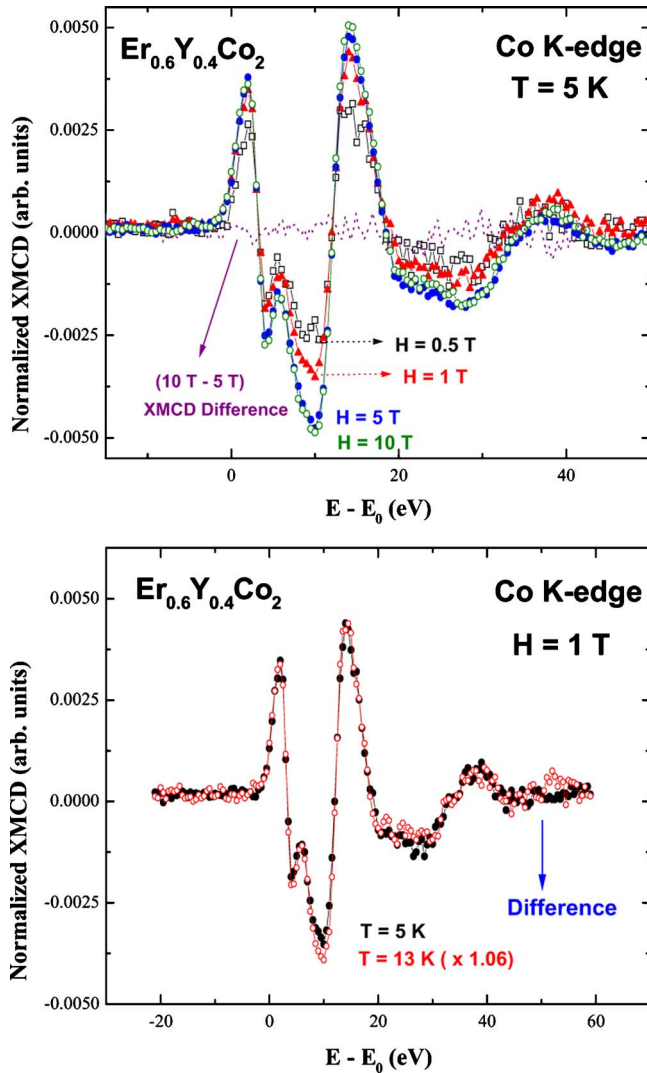
FIG. 7. (Color online) Comparison of the Co K-edge XMCD spectra of $Er_{0.6}Y_{0.4}Co_2$ recorded at $T=5$ K and different applied magnetic fields: $\mu_0H=0.5$ T (black, □), 1 T (red, △), 5 T (blue, •), and 10 T (green, ○). The dotted line (purple) corresponds to the difference of the XMCD spectra recorded at 10 T and 5 T. In the bottom panel the XMCD spectra of $Er_{0.6}Y_{0.4}Co_2$ recorded with a $\mu_0H=1$ T applied at $T=5$ K (black, •) and $T=13$ K (red, ○) are compared.

in $ErCo_2$ than in $Lu(Co_{0.9}Al_{0.1})_2$ for an applied field of $\mu_0H=10$ T. Moreover, even for a low 0.5-T applied field, the amplitude of the $ErCo_2$ signal is twice of that of the Lu compound recorded at 10 T. These differences cannot be ascribed to the magnitude of μ_{Co}, being of the same order ($\sim 0.7\mu_B - 0.9\mu_B$) in both compounds. As discussed above, the XMCD signal is mainly due to the Er magnetic contribution even when Co is probed by tuning its K-edge absorption edge.

The similar behavior is observed for the Y-doped $ErCo_2$ samples. Figure 7 shows the magnetic field dependence of the Co K-edge XMCD in the case of $Er_{0.6}Y_{0.4}Co_2$ recorded at low temperature. The spectral shape is the same as for $ErCo_2$, and only its amplitude is concerned, being the observed modification of the intensity in agreement with the magnetization data. In addition, the XMCD amplitude of $Er_{0.6}Y_{0.4}Co_2$ is similar for applied magnetic fields of $\mu_0H=5$ T and 10 T. This result indicates that, contrary to previous claims,[4,10,13] no inverse IEM transition occurs up to applied magnetic fields of $\mu_0H=10$ T. Indeed, if the Co moment collapses by increasing the external field, no Co contribution would be present in the XMCD spectrum recorded at 10 T. Consequently, the substraction of the XMCD

signals recorded at $\mu_0H=5$ T and 10 T, shown in Fig. 7, would be not zero but correspond to the Co contribution at $\mu_0H=5$ T. This signal would be similar to that of the $Y(Co_{0.85}Al_{0.15})_2$ and $Lu(Co_{0.9}Al_{0.1})_2$ compounds shown in Fig. 6. By contrast, the Co K-edge XMCD data indicate that the Co magnetic state is similar at both applied fields without an inverse IEM being detected.

More important to our aim is the comparison of the XMCD signals of $Er_{0.6}Y_{0.4}Co_2$ recorded at different temperatures shown in the bottom panel of Fig. 7. According to magnetization data (Fig. 2), the amplitude of the spectrum recorded at $T=13$ K has been factorized by 1.06 to account for the different magnetization of the Er sublattice at both temperatures. No appreciable difference between both signals is found, which points out that the Co sublattice orders at the same temperature as the Er one does in this compound. Indeed, magnetization data indicates that $\mu_{Co} \sim 0.55\mu_B$ in $Er_{0.6}Y_{0.4}Co_2$ at $T=5$ K. If the Co sublattice is not magnetically ordered at $T=13$ K, the difference reported in Fig. 7 would correspond to the XMCD signal of a RCo_2 compound without a magnetic rare earth, as the Er contribution is canceled by the substraction, and showing a $\mu_{Co} \sim 0.5\mu_B$. Consequently, the difference would exhibit a similar shape and

an intermediate amplitude between those of $Y(Co_{0.85}Al_{0.15})_2$ ($\mu_{Co} \sim 0.2 \mu_B$) and $Lu(Co_{0.9}Al_{0.1})_2$ ($\mu_{Co} \sim 0.7 \mu_B$) depicted in Fig. 6. Such a signal would be easily detectable. However, it is not observed in the present experimental spectra, which indicates that the Co sublattice is magnetically ordered at both temperatures.

Finally, we have faced the problem of confirming the existence of an average Co moment in the case of $Er_{0.5}Y_{0.5}Co_2$ for which different and contradictory results are given in literature. To this aim we have applied a two-sublattice model to account for the Co K-edge XMCD spectrum, as previously applied to the R-Fe case.[22–26] According to this model, it is assumed that the XMCD corresponds to the addition of the contribution of the magnetic Co sublattice and of the Er one, the latter being proportional to the number of neighboring Er atoms around absorbing Co. In order to verify this hypothesis, we have compared the Co K-edge XMCD spectra of compounds with a different Er-Y content. If our hypothesis is right, the amplitude of the Er contribution in $Er_{0.6}Y_{0.4}Co_2$ and $Er_{0.5}Y_{0.5}Co_2$ would be reduced by a factor of 0.6 and 0.5, respectively, with respect to that of $ErCo_2$. Consequently, we have scaled by a 0.6 (0.5) factor the XMCD signals of $Er_{0.6}Y_{0.4}Co_2$ ($Er_{0.5}Y_{0.5}Co_2$), to renormalize their Er contribution to that of the $ErCo_2$ XMCD. As shown in Fig. 8, after applying this procedure the three signals perfectly match in the high energy region—i.e., where the Er contribution is maximum. Differences are only found in the low-energy region—i.e., where the Co contribution is expected to be according to the XMCD of both Y and Lu compounds. Hence, the signal obtained after subtracting the above renormalized XMCD of $Er_{0.6}Y_{0.4}Co_2$ and $Er_{0.5}Y_{0.5}Co_2$ to the XMCD of $ErCo_2$ would correspond to the different Co magnetism in the three samples. The difference signals obtained in this way are shown in the bottom panel of Fig. 8. They exhibit the characteristic two-peak spectral feature of the Co K-edge XMCD of both $Y(Co_{0.85}Al_{0.15})_2$ and $Lu(Co_{0.9}Al_{0.1})_2$, supporting the conjecture that the signal extracted according the method above is related exclusively to the Co contribution to the XMCD. Then, we have applied the same method to the case of $Er_{0.6}Y_{0.4}Co_2$ and $Er_{0.5}Y_{0.5}Co_2$ compounds. In this way, the XMCD signal of $Er_{0.5}Y_{0.5}Co_2$ has been multiplied by 1.2 (0.6/0.5) to recover the same Er contribution as for $Er_{0.6}Y_{0.4}Co_2$. As shown in Fig. 9, there is a perfect coincidence of both signals for energies higher than 12 eV, and their difference shows at low energy the Co-like two-peak spectral profile. The extracted difference is related to that of the Co magnetic moment in both compounds in the form $\mu_{Co}|_{0.6} - 1.2 \times \mu_{Co}|_{0.5}$, where $\mu_{Co}|_{0.6}$ and $\mu_{Co}|_{0.5}$ are the μ_{Co} in $Er_{0.6}Y_{0.4}Co_2$ and $Er_{0.5}Y_{0.5}Co_2$, respectively. The amplitude of the difference signal is the same as for the Co K-edge XMCD spectrum of $Y(Co_{0.85}Al_{0.15})_2$ recorded at $\mu_0 H = 5$ T. For the latter compound $M(H)$ data yield a Co magnetic moment value of $\mu_{Co} = 0.22 \mu_B$. Then, by using this value and by considering that from magnetization data $\mu_{Co}|_{0.6} = 0.55 \mu_B$, this analysis yields $\mu_{Co}|_{0.5} = 0.28 \mu_B$. Consequently, the Co K-edge XMCD data indicate, in agreement with the Er $L_{2,3}$ study, that there is also a non-negligible magnetic moment at the Co sites in $Er_{0.5}Y_{0.5}Co_2$.
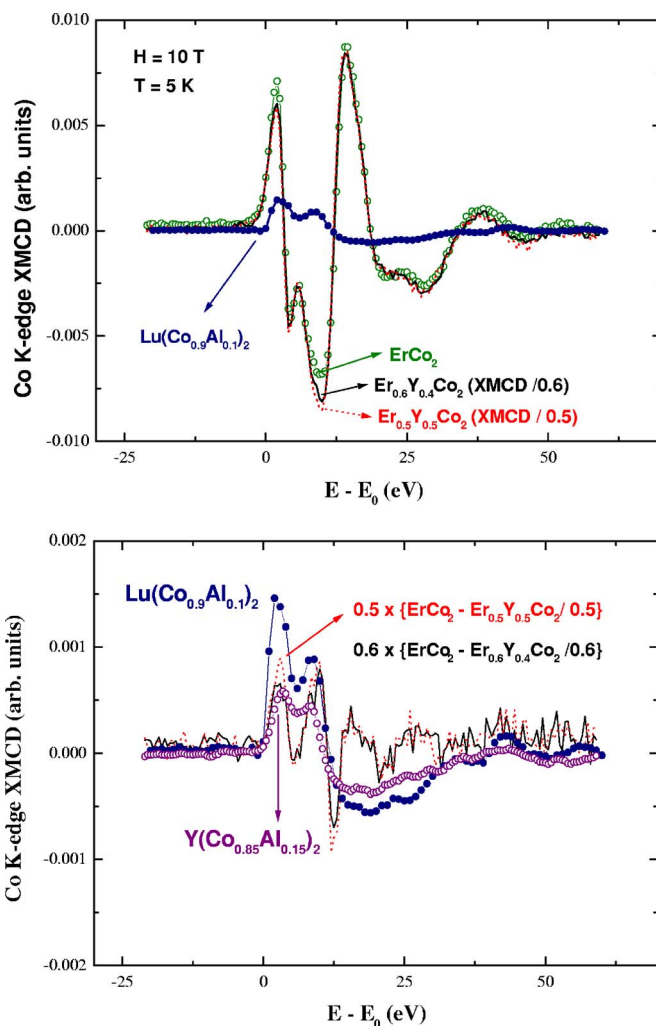

FIG. 8. (Color online) Top panel: comparison of Co K-edge XMCD spectra recorded at $T = 5$ K and $\mu_0 H = 10$ T of $Lu(Co_{0.9}Al_{0.1})_2$ (navy, •) and $ErCo_2$ (green, ○) to those of $Er_{0.6}Y_{0.4}Co_2$ (black, solid line) and $Er_{0.5}Y_{0.5}Co_2$ (red, dotted line) renormalized to the Er contribution (see text for details). Bottom panel: comparison of Co K-edge XMCD spectra of $Lu(Co_{0.9}Al_{0.1})_2$ (navy, •) and $Y(Co_{0.85}Al_{0.15})_2$ (purple, ○) to the difference between the $ErCo_2$ XMCD and the renormalized signals of $Er_{0.6}Y_{0.4}Co_2$ (black, solid line) and $Er_{0.5}Y_{0.5}Co_2$ (red, dotted line) (see text for details).

IV. SUMMARY AND CONCLUSIONS

We have reported here a systematic XMCD study performed at the Co K edge and at the Er $L_{2,3}$ edges in the $Er_{1-x}Y_xCo_2$ series as a function of the yttrium concentration, the applied magnetic field, and the temperature.

In the case of the $Er_{0.6}Y_{0.4}Co_2$ compounds, XMCD data do not show the decoupling of the magnetic ordering for both Er and Co sublattices. In addition, no experimental evidence of the occurrence of an inverse IEM has been found for applied magnetic fields of up to $\mu_0 H = 10$ T. In addition, a nonzero magnetic moment is found at the Co sites in the case of the $Er_{0.5}Y_{0.5}Co_2$ compound.

Our results shed light on the current debate existing on the magnetic behavior of the $Er_{1-x}Y_xCo_2$ systems for yttrium

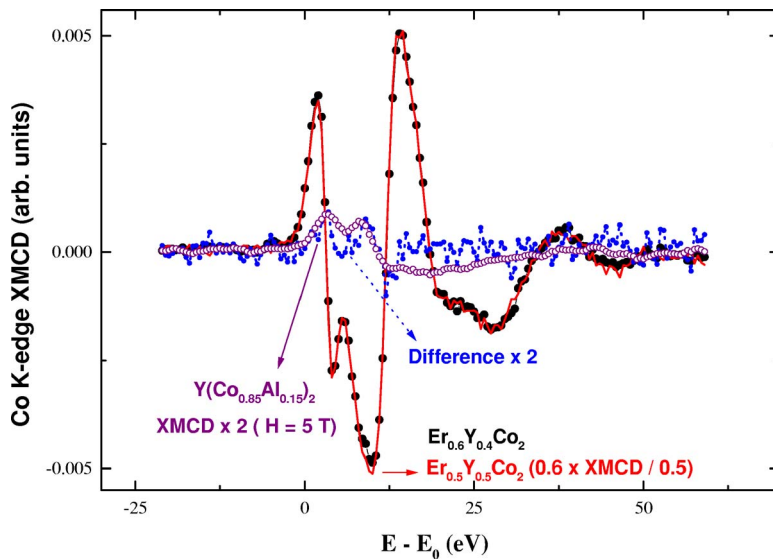FIG. 9. (Color online) Top panel: comparison of Co K-edge XMCD spectra of $Er_{0.6}Y_{0.4}Co_2$ recorded at $T=5$ K and $\mu_0H=10$ T (black, •) and that of $Er_{0.5}Y_{0.5}Co_2$ (red, dotted line) renormalized to the Er contribution (see text for details). Its difference (blue, dots) is compared to the XMCD of $Y(Co_{0.85}Al_{0.15})_2$ (purple, ○) recorded at the same temperature and $\mu_0H=5$ T.

concentrations close to the critical one for the existence of long-range magnetic order.[6–12,14] This XMCD study will contribute to a better understanding of the nature of both IEM and inverse IEM metamagnetic transitions in itinerant-electron R-Co systems and in the modification of the effective field acting on the Co subsystem by diluting the magnetic rare-earth ions.

[1] J. J. M. Franse and R. J. Radwanski, in *Handbook on Magnetic Materials*, edited by K. H. J. Buschow (Elsevier Science, Amsterdam, 1993), Vol. 17, Chap. 5.

[2] N. H. Duc and P. E. Brommer, in *Handbook on Magnetic Materials*, edited by K. H. J. Buschow (Elsevier Science, Amsterdam, 1999), Vol. 12, Chap. 3.

[3] N. H. Duc and T. Goto, in *Handbook on the Physics and Chemistry of Rare Earths*, edited by K. A. Gscheider, Jr. and L. Eyring (Elsevier Science, Amsterdam, 1999), Vol. 26, Chap. 171.

[4] E. Gratz and A. S. Markosyan, J. Phys.: Condens. Matter **13**, R385 (2001).

[5] N. H. Duc, T. D. Hien, P. E. Brommer, and J. J. M. Franse, J. Phys. F: Met. Phys. **18**, 275 (1988).

[6] N. V. Baranov, A. I. Kozlov, A. N. Pigorov, and E. V. Sinitsyn, Sov. Phys. JETP **69**, 382 (1989).

[7] R. Hauser, E. Bauer, E. Gratz, M. Rotter, G. Hilscher, H. Michor, and A. S. Markosyan, Physica B **237-238**, 577 (1997).

[8] R. Hauser, E. Bauer, E. Gratz, M. Rotter, H. Müller, G. Hilscher, H. Michor, and A. S. Markosyan, Physica B **239**, 83 (1997).

[9] R. Hauser, E. Bauer, E. Gratz, H. Müller, M. Rotter, H. Michor, G. Hilscher, A. S. Markosyan, K. Kamishima, and T. Goto, Phys. Rev. B **61**, 1198 (2000).

[10] R. Hauser, C. Kussbach, R. Grössinger, G. Hilscher, Z. Arnold, J. Kamarad, A. S. Markosyan, E. Chappel, and G. Chouteau, Physica B **294&295**, 182 (2001).

[11] A. Podlesnyak, T. Strässle, A. Mirmelstein, A. Pirogov, and R. Sadykov, Eur. Phys. J. B **29**, 547 (2002).

[12] A. Podlesnyak, T. Strässle, J. Schefer, A. Furrer, A. Mirmelstein,

A. Pirogov, P. Markin, and N. Baranov, Phys. Rev. B **66**, 012409 (2002).

[13] A. S. Markosyan, R. Hauser, M. Galli, E. Bauer, E. Gratz, G. Hilscher, K. Kamishima, and T. Goto, J. Magn. Magn. Mater. **185**, 235 (1998).

[14] N. V. Baranov and A. N. Pigorov, J. Alloys Compd. **217**, 31 (1995).

[15] J. Rodriguez-Carvajal, Physica B **192**, 55 (1993).

[16] H. Maruyama, J. Synchrotron Radiat. **6**, 1133 (1999).

[17] M. Suzuki, N. Kawamura, M. Mizumaki, A. Urata, H. Maruyama, S. Goto, and T. Ishikawa, Jpn. J. Appl. Phys., Part 2 **37**, L1488 (1998).

[18] R. M. Moon, W. C. Koehler, and J. Farrel, J. Appl. Phys. **36**, 978 (1965).

[19] J. C. Lang, G. Srajer, C. Detlefs, A. I. Goldman, H. König, X. Wang, B. N. Harmon, and R. W. McCallum, Phys. Rev. Lett. **74**, 4935 (1995).

[20] H. G. Purwins, E. Walker, B. Barbara, M. F. Rossignol, and A. Furrer, J. Phys. C **9**, 1025 (1976).

[21] M. A. Laguna-Marco, J. Chaboy, C. Piquer, H. Maruyama, N. Ishimatsu, N. Kawamura, M. Takagaki, and M. Suzuki, Phys. Rev. B **72**, 052412 (2005).

[22] M. A. Laguna-Marco, J. Chaboy, and H. Maruyama, Phys. Rev. B **72**, 094408 (2005).

[23] J. Chaboy, H. Maruyama, L. M. García, J. Bartolomé, K. Kobayashi, N. Kawamura, A. Marcelli, and L. Bozukov, Phys. Rev. B **54**, R15637 (1996).

[24] J. Chaboy, L. M. García, F. Bartolomé, H. Maruyama, A. Mar-

celli, and L. Bozukov, Phys. Rev. B **57**, 13386 (1998).

[25] J. Chaboy, C. Piquer, N. Plugaru, M. Artigas, H. Maruyama, N. Kawamura, and M. Suzuki, J. Appl. Phys. **93**, 475 (2003).

[26] J. Chaboy, M. A. Laguna-Marco, M. C. Sánchez, H. Maruyama, N. Kawamura, and M. Suzuki, Phys. Rev. B **69**, 134421 (2004).

[27] J. P. Rueff, R. M. Galéra, C. Giorgetti, E. Dartyge, C. Brouder, and M. Alouani, Phys. Rev. B **58**, 12271 (1998).

[28] M. A. Laguna-Marco, J. Chaboy, C. Piquer, H. Maruyama, N. Kawamura, and M. Takagaki, J. Magn. Magn. Mater. (to be published).

[29] M. L. Fdez-Gubieda, A. García-Arribas, J. M. Barandiarán, R. López Antón, I. Orue, P. Gorria, S. Pizzini, and A. Fontaine, Phys. Rev. B **62**, 5746 (2000).